◆ Human Brain Mapping 35:4693–4705 (2014) ◆

Disrupted Network Architecture of the Resting Brain in Attention-Deficit/Hyperactivity Disorder

Chandra Sripada,[1]* Daniel Kessler,[1] Yu Fang,[1] Robert C. Welsh,[1,2] Krishan Prem Kumar,[1] and Michael Angstadt[1]

[1]*Department of Psychiatry, University of Michigan, Ann Arbor, Michigan*
[2]*Department of Radiology, University of Michigan, Ann Arbor, Michigan*

Abstract: *Background:* Attention-deficit/hyperactivity disorder (ADHD) is one of the most prevalent psychiatric disorders of childhood. Neuroimaging investigations of ADHD have traditionally sought to detect localized abnormalities in discrete brain regions. Recent years, however, have seen the emergence of complementary lines of investigation into distributed connectivity disturbances in ADHD. Current models emphasize abnormal relationships between default network—involved in internally directed mentation and lapses of attention—and task positive networks, especially ventral attention network. However, studies that comprehensively investigate interrelationships between large-scale networks in ADHD remain relatively rare. *Methods:* Resting state functional magnetic resonance imaging scans were obtained from 757 participants at seven sites in the ADHD-200 multisite sample. Functional connectomes were generated for each subject, and interrelationships between seven large-scale brain networks were examined with network contingency analysis. *Results:* ADHD brains exhibited altered resting state connectivity between default network and ventral attention network [$P < 0.0001$, false discovery rate (FDR)-corrected], including prominent increased connectivity (more specifically, diminished anticorrelation) between posterior cingulate cortex in default network and right anterior insula and supplementary motor area in ventral attention network. There was distributed hypoconnectivity within default network ($P = 0.009$, FDR-corrected), and this network also exhibited significant alterations in its interconnections with several other large-scale networks. Additionally, there was pronounced right lateralization of aberrant default network connections. *Conclusions:* Consistent with existing theoretical models, these results provide evidence that default network-ventral attention network interconnections are a key locus of dysfunction in ADHD. Moreover, these findings contribute to growing evidence that distributed dysconnectivity within and between large-scale networks is present in ADHD. *Hum Brain Mapp 35:4693–4705, 2014.*

Key words: attention-deficit/hyperactivity disorder; functional magnetic resonance imaging; resting state connectivity; default network; ventral attention network; frontoparietal network; connectomics; ADHD-200

Contract grant sponsor: National Center for Advancing Translational Sciences of the National Institutes of Health; Contract grant number: UL1TR000433; Contract grant sponsor: NIH; Contract grant number: AA020297; Contract grant sponsors: Center for Computational Medicine Pilot Grant, and the John Templeton Foundation (to CS).

*Correspondence to: Chandra Sripada, Department of Psychiatry, University of Michigan, Rachel Upjohn Building, Room 2743, 4250 Plymouth Road, Ann Arbor, Michigan 48109. E-mail: sripada@umich.edu

Chandra Sripada and Daniel Kessler contributed equally.

Received for publication 21 September 2013; Revised 15 January 2014; Accepted 24 February 2014.

DOI 10.1002/hbm.22504

Published online 25 March 2014 in Wiley Online Library (wileyonlinelibrary.com).

INTRODUCTION

Attention-deficit/hyperactivity disorder (ADHD) is neurodevelopmental disorder characterized by age-inappropriate inattention, hyperactivity, and impulsivity (American Psychiatric Association et al., 2013). The disorder affects 5–8% of children (Polanczyk and Rohde, 2007), frequently persists into adulthood (Kessler et al., 2006), and produces significant academic, psychosocial, and economic impairment (Harpin, 2005). The neurobiological mechanisms of the disorder, however, remain poorly understood. Neuroimaging investigations of ADHD have traditionally sought to detect localized abnormalities in discrete brain regions, such as areas associated with motor inhibition (Aron and Poldrack, 2005) and cognitive control (Bush et al., 1999). Recent years have seen the emergence of complementary lines of investigation into distributed connectivity disturbances in ADHD (Cortese et al., 2013; van Ewijk et al., 2012), bringing a new network perspective to understanding the pathophysiology of the disorder (Bush, 2009; Castellanos and Proal, 2012).

It is increasingly recognized that the human brain is organized into large-scale intrinsic connectivity networks (ICNs; Fox et al., 2005; Power et al., 2011; Sporns et al., 2004). These are distributed brain regions that exhibit coherent activity, and which are reliably detected (Damoiseaux et al., 2006; Shehzad et al., 2009) from low-frequency oscillations of the blood oxygenation level-dependent (BOLD) signal during the resting state. Individual ICNs have been implicated in specific neurocognitive functions such as visual, somatomotor, attention, and executive processing (Bressler and Menon, 2010; Laird et al., 2011; Smith et al., 2009). Moreover, aberrant connectivity within and between ICNs has been discovered in a number of psychiatric conditions (Hamilton et al., 2011; Menon, 2011; Sripada et al., 2012; Tu et al., 2013).

In ADHD, theoretical models of network pathology in the disorder have focused on default network and its interrelationships with task-positive ICNs (Castellanos and Proal, 2012; Sonuga-Barke and Castellanos, 2007). The default network consists of interconnected midline and lateral parietal regions and is involved in internally directed mentation (Buckner et al., 2008; Raichle et al., 2001). Externally directed cognitive tasks are supported by several task-positive ICNs, with ventral attention network (often called "salience network") thought to be responsible for regulating shifts between externally focused and internally directed mentation (Menon, 2011; Menon and Uddin, 2010). Intrusion of default network during externally focused tasks, possibly due to ineffective regulation by ventral attention network, leads to lapses of attention (Sonuga-Barke and Castellanos, 2007; Weissman et al., 2006). A recent activation likelihood estimation meta-analysis of task-based activation studies in ADHD found abnormal activation in regions associated with ventral attention network and default network, leading to the conjecture of altered connectivity patterns between these networks in the disorder (Cortese et al., 2012). Indeed, seed-based connectivity studies in ADHD do find abnormal connectivity patterns using ventral attention and default mode seeds (Castellanos et al., 2008; Tian et al., 2006). These studies, however, have often involved small samples, have examined connectivity at different individual seed regions making comparisons difficult, and have produced somewhat inconsistent results (see Konrad and Eickhoff, 2010 for a review). Studies in ADHD with large samples that that have comprehensively examined connectivity abnormalities across the complete range of large-scale brain networks remain relatively rare.

Our aim in this study was to fill this gap by investigating aberrant relationships within and between seven major ICNs in childhood ADHD. We used two methods to substantially enhance the scope and reliability of our findings. First, previous studies have demonstrated the fruitfulness of aggregating resting state scans across multiple data collection sites, producing increases in sample size and concomitant increases in power and reliability of statistical inferences (Anderson et al., 2011; Biswal et al., 2010; Fair et al., 2013). Thus, we utilized the ADHD-200 database, which includes more than 750 scans drawn from multiple sites (ADHD-200 Consortium, 2012). Second, previous studies in ADHD have often used seed-based methods to investigate functional connectivity (e.g., Castellanos et al., 2008; Tian et al., 2006). These methods have the advantage of identifying connectivity changes at well-defined regions. They are, however, restricted to investigating a single or handful of selected regions and require potentially arbitrary choices of which a priori regions to investigate. Additionally, when inferences about networks are made, they require the assumption that the connectivity patterns of entire networks are faithfully reflected in the connectivity patterns of individual seeds. In the present study, we comprehensively investigated connectivity disturbances by placing 907 regions of interest (ROIs) at regular intervals throughout the entire neocortex. We used a network-based analysis approach that identifies abnormalities across all seven major ICNs and their interconnections (Sripada et al., 2013, 2014). While we were interested in comprehensively characterizing network abnormalities throughout the cortex, based on recently proposed network models of ADHD (Castellanos and Proal, 2012; Sonuga-Barke and Castellanos, 2007), we had strong a priori hypotheses that ADHD participants would exhibit abnormal connectivity between default network and task positive ICNs, in particular ventral attention network.

METHODS

Subjects

A total of 757 participants underwent resting state scanning at seven contributing sites: New York University Child Study Center, Beijing Normal University, University

TABLE I. Sample characteristics of the ADHD-200 dataset

	Healthy controls				ADHD			
Site	*n*	Age	% Male	IQ	*n*	Age	% Male	IQ
Pre-exclusions								
NYU	93	12.1 ± 3.1	45.2	110.7 ± 13.9	116	11.3 ± 2.7	77.6	106.4 ± 14.0
Beijing	116	11.7 ± 1.7	61.2	118.1 ± 13.3	78	12.4 ± 2.0	91.0	105.4 ± 13.2
Pittsburgh	89	15.1 ± 2.9	51.7	109.8 ± 11.5	NA			
OHSU	41	8.9 ± 1.2	43.9	118.7 ± 12.6	37	8.8 ± 1.0	70.3	108.5 ± 13.9
NeuroImage	22	17.3 ± 2.6	50.0	111.2	23	16.7 ± 3.0	82.6	111.2
Washington	59	11.5 ± 3.9	52.5	116 ± 14.1	NA			
KKI	61	10.3 ± 1.3	55.7	111.5 ± 10.3	22	10.2 ± 1.6	54.6	106.0 ± 15.2
Total	481	12.2 ± 3.3	52.9	113.7 ± 12.9	276	11.6 ± 3.0	79.1	106.8 ± 13.3
Postexclusions								
NYU	49	12.7 ± 2.9	44.9	113.6 ± 11.8	52	11.7 ± 3.1	71.2	107.5 ± 12.9
Beijing	89	11.8 ± 1.8	58.4	118.1 ± 11.9	47	12.5 ± 2.1	91.5	105.8 ± 12.5
Pittsburgh	54	15.7 ± 2.8	48.2	113.1 ± 9.9	NA			
OHSU	19	9.2 ± 1.5	47.4	116.6 ± 12.5	15	9.2 ± 1.3	73.3	112.3 ± 12.5
NeuroImage	15	16.0 ± 2.4	46.7	111.2	9	16.1 ± 2.4	88.9	111.2
Washington	24	13.8 ± 4.1	45.8	114.9 ± 11.2	NA			
KKI	38	10.5 ± 1.3	55.3	111.2 ± 11.5	10	11.1 ± 1.7	60	100.8 ± 14.4
Total	288	12.8 ± 3.2	51.4	114.8 ± 11.3	133	12.0 ± 2.9	79.0	107.2 ± 12.5

ADHD, attention-deficit/hyperactivity disorder; NYU, New York University; OHSU, Oregon Health and Science University; KKI, Kennedy Krieger Institute.
Sample characteristics are shown both prior to and after application of exclusion and quality control criteria.

of Pittsburgh, Oregon Health and Science University, NeuroImage, Washington University at St. Louis, and Kennedy Krieger Institute. The dataset comprised 481 typically developing control participants and 276 participants with a Diagnostic and Statistical Manual of Mental Disorders (Fifth Edition, Text Revision) diagnosis of ADHD. A summary of the demographic characteristics for each site is provided in Table I. Informed consent was obtained from all participants, and procedures complied with the respective Human Investigation Review Boards. Detailed reporting of ADHD assessment protocols is available elsewhere (Fair et al., 2013).

Data Acquisition

All participants were scanned on 3.0 T scanners using standard resting connectivity T2*-weighted echo-planar imaging. All imaging data used is publicly available at the Neuroimaging Informatics Tools and Resources Clearinghouse, see http://fcon_1000.projects.nitrc.org/indi/adhd200. See the ADHD-200 website and Fair et al. (2013) for detailed reporting of data provenance, complete phenotypic information, scanner acquisition parameters, contributing principal investigators, and funding sources.

Imaging Sample Selection

Analyses were limited to participants with: (1) MPRAGE anatomical images, with consistent nearfull brain coverage (i.e., superior extent included the majority of frontal and parietal cortex and inferior extent included the temporal lobes) with successful registration; (2) complete phenotypic information for main phenotypic variables (diagnosis, age, handedness), though imputation was allowed for missing intelligence quotient (IQ) data (see subsequently); (3) full IQ (FIQ) within two standard deviation (SD) of the overall ADHD-200 sample mean, (4) mean framewise displacement (FD) within two SD of the ADHD-200 sample mean; (5) at least 40% of frames retained after application of framewise censoring for motion ("motion scrubbing"; see subsequently).

After applying these sample selection criteria, we analyzed resting state scans from 421 individuals [healthy control (HC) = 288; ADHD = 133] from seven sites. Demographic characteristics of the postexclusion sample are shown in Table I. Of note, for participants lacking a F4 or F2 IQ score, FIQ was estimated by averaging the participant's performance and verbal IQ scores. For the NeuroImage site which lacked IQ information, the mean IQ across the other sites was imputed.

Preprocessing

Preprocessing steps were performed using statistical parametric mapping (SPM8; http://www.fil.ion.ucl.ac.uk/spm). Scans were slice-time corrected, realigned to the first scan in the experiment for correction of head motion, and coregistered with the high-resolution T1-weighted image.

Normalization was performed using the voxel-based morphometry toolbox implemented in SPM8. The high-resolution T1-weighted image was segmented into tissue types, bias-corrected, registered to MNI space, and then normalized using Diffeomorphic Anatomical Registration Through Exponentiated Lie Algebra (Ashburner, 2007). The resulting deformation fields were then applied to the functional images. Smoothing of functional data was performed with an 8 mm^3 kernel.

Connectome Generation

In order to produce a whole-brain resting state functional connectome, we placed ROIs encompassing nineteen $3 \times 3 \times 3$ mm voxels in a regular grid spaced at 12 mm intervals throughout the brain. Each ROI consisted of a $3\sqrt{2}$ mm (i.e., roughly 4.24 mm) voxel center-to-voxel center radius pseudosphere. Given our 8 mm smoothing kernel, this density of sampling also ensured that information from the entirety of brain was comprehensively sampled. Of note, our placement of seed ROIs densely throughout the brain introduces redundancy as closely spaced seed ROIs will yield highly similar connectivity maps, which in turn raises concern about needless multiple comparisons. However, the network contingency statistic we introduce below obviates this issue, as the number of comparisons is based on the number of ICNs investigated (i.e., 7), rather than the number of seed ROIs. Since our main interest was cortical ICNs, we next removed all ROIs that fell more than 5 mm (Euclidean distance) from the Yeo et al. (2011) ICN parcellation of the brain, yielding 907 ROIs in total. We chose the Yeo and colleagues network map because their study was based on a large number of subjects (1,000 participants), they included multiple convergent methods to assess reliability, and their parcellation was derived using grid-based connectomic methods similar to the current study.

Spatially averaged time series were next extracted from each of the ROIs. Next, regression was performed to remove nuisance effects. Regressors included six motion regressors generated from the realignment step, as well as their first derivatives. White matter and cerebrospinal fluid masks were generated from the VBM-based tissue segmentation step noted above, and eroded using the fslmaths program from FSL to eliminate border regions of potentially ambiguous tissue type. The top five principal components of the BOLD time series were extracted from each of the masks and included as regressors in the model—a method that has been demonstrated to effectively remove signals arising from the cardiac and respiratory cycle (Behzadi et al., 2007).

The time series for each ROI was next band-passed filtered in the 0.01–0.10 Hz range. Next, motion scrubbing was performed. Individual frames with excessive head motion were censored from the time series. The FD threshold for excessive motion was set at 0.2 mm (Fair et al., 2013). One frame before and two frames after the target frame were also removed to account for temporal blurring (Power et al., 2012). Subjects with more than 60% of their frames removed by scrubbing were excluded from further analysis, a threshold justified by simulations conducted by other groups (Fair et al., 2013), as well as by our group.

Pearson's product–moment correlation coefficients were then calculated pairwise between time courses for each of the 907 ROIs, producing a cross-correlation map with 410,871 nonredundant entries. Fisher's r–z transformation was then applied.

Network Contingency Analysis

Our main aim was to determine whether and where patterns of ICN connectivity significantly differed in ADHD versus HCs. To address this issue, we performed a network contingency analysis. This analysis takes a population-based approach to the question of when two networks exhibit disrupted connectivity. In particular, it addresses the question of whether for the set of edges linking two large-scale networks, the population of disease-modulated edges is larger than one would expect by chance. This analysis method has a number of advantages compared to alternatives. First, this method is applied to connectomes that represent patterns of connectivity across the entire brain, and does not require potentially arbitrary choices of seed regions. Second, this method leverages a priori information about network structure to directly assess questions about internetwork connectivity. Third, it avoids univariate tests across the hundreds of thousands of connections of the connectome, instead conducting a single statistical test for each network pair investigated. Fourth, it uses permutation tests, a nonparametric test that is robust to deviations from assumptions of normality and independence. Network contingency analysis is composed of the following three steps (see Fig. 1 for an overview).

Step 1. Subtraction and thresholding: We subtracted the mean ADHD connectome from the mean HC connectome, producing a ADHD–HC delta connectome, and we thresholded this delta connectome based on statistical significance at $P < 0.001$ (the rationale for this threshold is discussed subsequently). More specifically, this subtraction was performed in a multiple regression framework. For each edge, we fit a multiple regression model that modeled the effect of disease (ADHD versus HC), while controlling for the effects of site, gender, age, full-scale IQ, and handedness. We also included terms modeling the linear and quadratic effects of mean motion (FD averaged across the entire scan) to absorb any residual variance unaccounted for by the previously mentioned motion correction steps (i.e., removal of high motion subjects, regression of motion from the resting state time series, and scrubbing of high motion frames).

Step 2. Organize edges based on network affiliation: We next organized the suprathreshold edges of the ADHD–HC delta connectome in terms of network affiliation. We

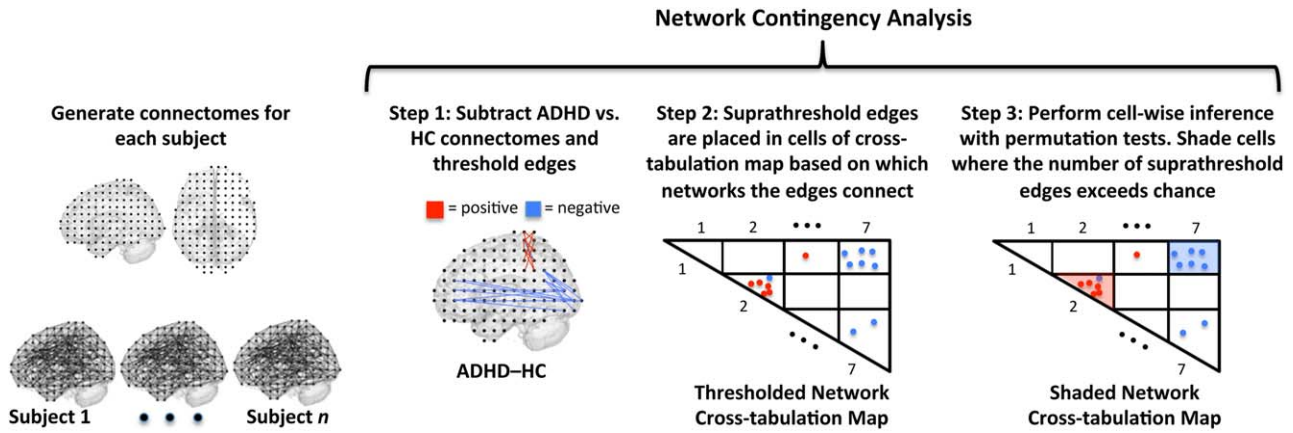

Figure 1.

Steps of the network contingency analysis. All possible interconnections between seven major intrinsic connectivity networks are represented in 28 (nonredundant) cells of a network cross-tabulation map. The network contingency analysis takes a population-based approach to the question of when two networks exhibit disrupted connectivity. For each cell, the analysis assesses whether the number of disease-modulated edges is greater than would be expected by chance. Each step of the analysis is discussed in greater detail in the main text. ADHD, attention-deficit/hyperactivity disorder; HC, healthy control. [Color figure can be viewed in the online issue, which is available at wileyonlinelibrary.com.]

utilized the network map of Yeo et al. (2011) discussed above which parcellates the brain into seven major networks. These seven networks were used to generate a cross-tabulation map with 28 nonredundant cells (Fig. 1), with each cell representing the set of edges linking two networks.

Step 3. Cell-wise contingency analysis: We tested the hypothesis that the number of observed suprathreshold edges in each cell of the network cross-tabulation map exceeds the number that would be expected by chance alone. The distribution under chance of observed edges for each cell was generated by randomly permuting the disease labels (HC versus ADHD) of the 421 participants 10,000 times, and counting the number of suprathreshold edges in each cell at each permutation (Good, 2000). Since the model includes covariates, the procedure of Freedman and Lane (1983) was followed (see FSL Randomise http://fsl.fmrib.ox.ac.uk/fsl/fslwiki/Randomise/Theory for a neuroimaging implementation).

We performed a cell-wise contingency analysis separately for each cell of the thresholded network cross-tabulation map and corrected for multiple comparisons with the false discovery correction procedure [false discovery rate (FDR); Benjamini and Hochberg, 1995]. Cells that survived FDR correction were next shaded. Since we were also interested in the directionality of changes, the cell was shaded more red as the proportion of suprathreshold cells that exhibit positive change approaches one and more blue as this number approaches zero (predominantly negative changes).

In order to clarify location, distribution, and lateralization of implicated edges, we generated three-dimensional visualizations of the statistically significant cells from Step 3 using BrainNet Viewer, http://www.nitrc.org/projects/bnv/ (Xia et al., 2013). Because visual inspection of these 3-dimensional renderings suggested lateralization of network abnormalities, we conducted Bernoulli tests to identify statistically significant differences in the number of edges on the right versus left side of networks (i.e., number of edges on the right was compared with a binomial distribution $B(p,n)$, with $P = 0.5$ and n=421 samples). Since nine post hoc statistical tests were performed, we used Bonferroni correction for multiple comparisons. Of note, since we controlled for the effects of nuisance covariates in Step 1 of the network contingency analysis (see above), and performed Bernoulli tests for laterality only subsequently, we thus avoided the problems inherent in the traditional "laterality index" (Bullmore et al., 1995).

In Step 1 of the network contingency analysis, we set the P value threshold ("$p_{\text{threshold}}$") to be 0.001, consistent with prior studies (e.g., Di Martino et al., 2013). To test the robustness of the analysis under different threshold values, we performed the ADHD versus HC network contingency analysis with $p_{\text{threshold}}$ set to {0.0001, 0.0005, 0.001, 0.005, 0.01, 0.05, 0.1}. Each of these $p_{\text{threshold}}$ values yielded a P value map (one P value for each of the 28 cells that make up the map). We then generated a weighted mean of these P values across the thresholds by calculating a normalized area under the curve. In doing this calculation, the $p_{\text{threshold}}$ values were first z-transformed so that the distance between $p_{\text{threshold}}$ values was well scaled. This procedure yielded a single weighted mean P value map. We then performed FDR correction for multiple comparisons on these P values

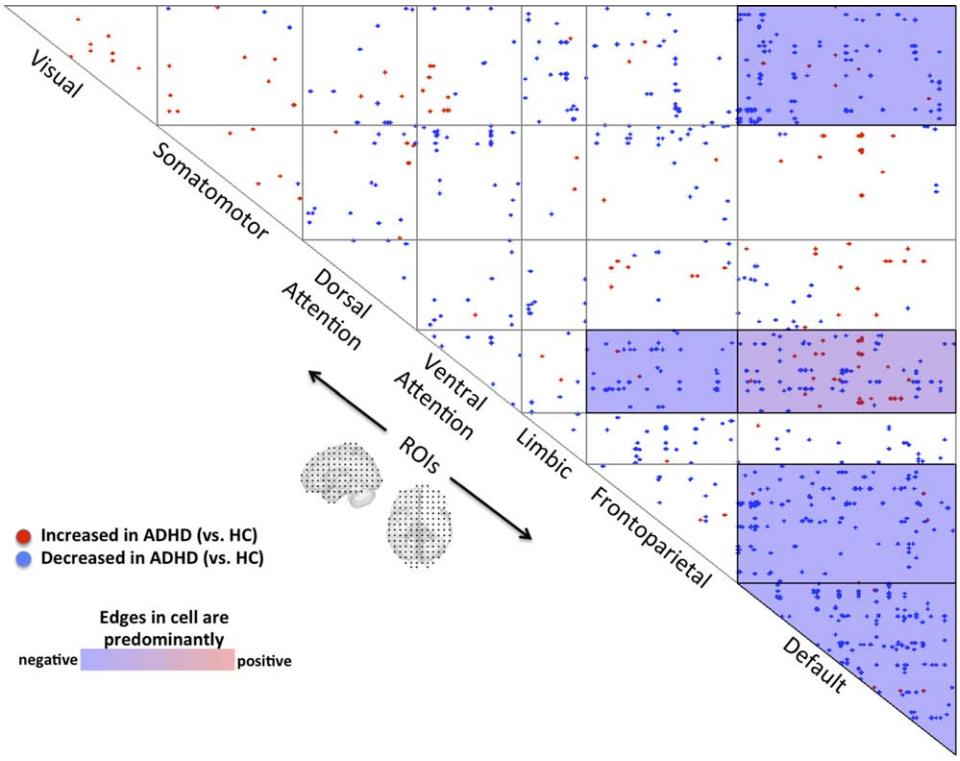

Figure 2.

Network cross-tabulation map. Network contingency analysis revealed significantly abnormal connectivity in ADHD brains in the following networks (shaded above): ventral attention–default, visual–default, frontoparietal–default, default–default, and ventral attention–frontoparietal. ADHD, attention-deficit/hyperactivity disorder; HC, healthy control. [Color figure can be viewed in the online issue, which is available at wileyonlinelibrary.com.]

and compared the results to those resulting from the analysis with $p_{\text{threshold}}$ set at 0.001.

Because we had a strong a priori hypothesis about abnormal connectivity between default network and ventral attention network, we performed a more detailed characterization of interconnections of these two networks. In particular, we generated circular connection graphs that allow appreciation of the spatial distribution across the subregions of default network and ventral attention network of the population of connections that strongly differ between HC and ADHD. To do this, we leveraged the fact that these ICNs are comprised of a number of spatially distinct subregions. More specifically, default network and ventral attention network were split into a number of distinct contiguous subregions using the "pick cluster" function in XJView. This yielded 13 large contiguous regions such as insula, posterior cingulate cortex, and supplementary motor area, many of which have right and left components (see Fig. 4). Of note, since anterior medial frontal cortex comprises a massive contiguous region that is commonly split into ventral and dorsal components (e.g., Amodio and Frith, 2006), we split this region at the MNI $z = 0$ line. We then created circular graphs in which these subregions are connected by arcs, where the width of arcs was computed as follows: Let P be the size of the population of connections linking default network and ventral attention network that strongly differ between HC and ADHD (after $P < 0.001$ thresholding of connectomic maps). Let L be the number of connections within this population that links a pair of subregions. The width of the arc connecting this pair of subregions was set to be proportional to L/P, and this procedure was repeated for all pairs of subregions. Of note, to enhance the readability of the circular graphs, arcs that represent less than 1% of the internetwork connections were omitted. In addition, if subregions participated in less than 1% of total connections, they were omitted from the graph (for regions with right and left components, we required that both sides participate in less 1% of connections).

In the postexclusion ADHD-200 sample, continuous measures of symptom severity were available for 265 participants (105 ADHD, 160 HC). In the cells that showed significant effects in the first network contingency analysis, we used these scores to perform an additional network contingency analysis in order to assess whether aberrant network interconnectivity varied as a function of symptom

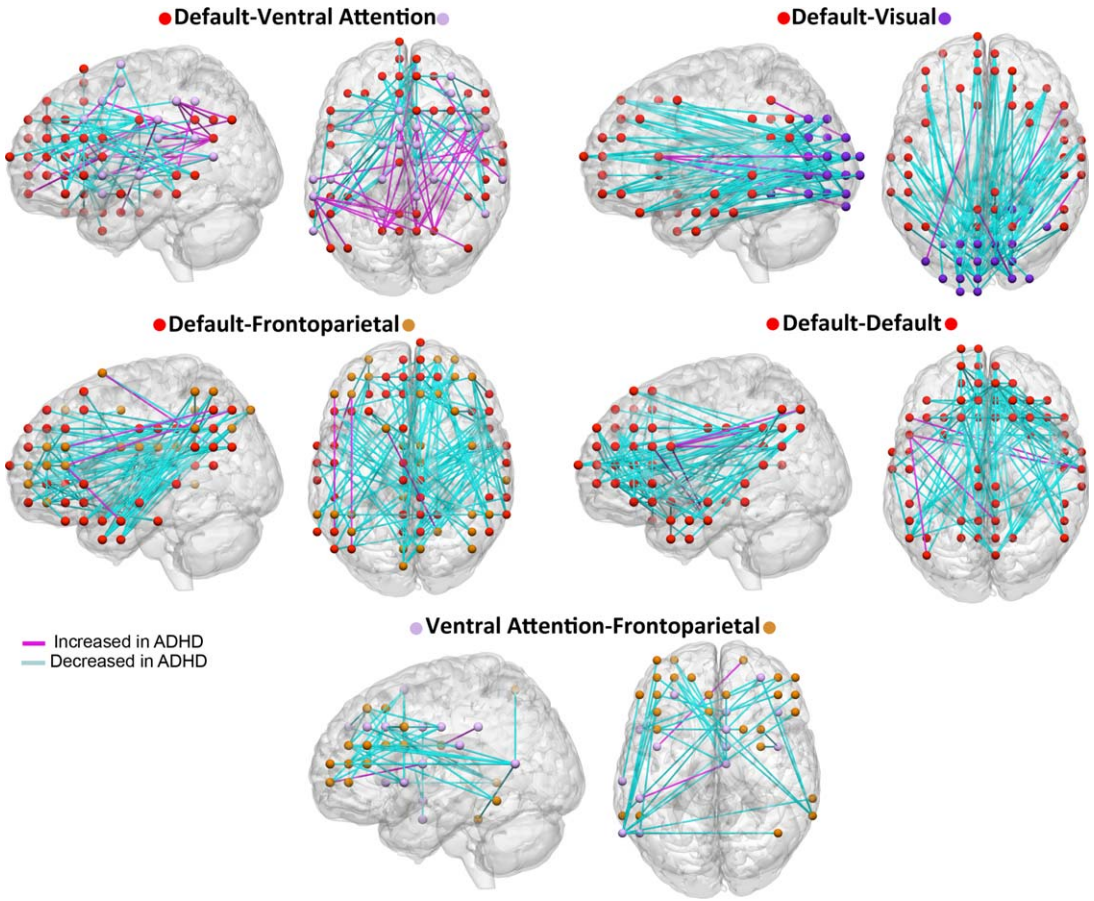

Figure 3.

3D visualization of abnormal network interconnections. ADHD brains exhibited abnormal network-to-network interconnections involving five network pairs. Each of these five sets of abnormal network-to-network interconnections is rendered separately on sagittal and axial views of a canonical brain. ADHD, attention-deficit/hyperactivity disorder. [Color figure can be viewed in the online issue, which is available at wileyonlinelibrary.com.]

load. More specifically, we reran Steps 1 through 3 above with the exception that continuous severity scores rather than categorical disease labels were included in the regression model. Because sample size was roughly halved, a more lenient $p_{\text{threshold}}$ value of 0.01 was utilized in Step 1 of the analysis.

RESULTS

Results from the main network contingency showed statistically significant effects in five cells (where each cell represents the set of connections linking two networks; see Fig. 2). Consistent with our a priori hypothesis, individuals with ADHD exhibited altered connectivity between ventral attention network and default network ($P < 0.0001$, FDR-corrected). In addition, in ADHD, there was diffuse hypoconnectivity within the default network ($P = 0.009$, FDR-corrected), and altered connectivity between default network and visual network ($P = 0.015$, FDR-corrected) as well as frontoparietal network ($P = 0.003$, FDR-corrected). Also, aberrant connectivity was observed between ventral attention network and frontoparietal network ($P = 0.017$, FDR-corrected). All five of these network pairs are shaded primarily blue in Figure 2, indicating there was a preponderance of edges exhibiting decreased connectivity in ADHD compared to HC. These five abnormal network interrelationships are rendered three-dimensionally on sagittal and axial views of a canonical brain in Figure 3.

Since our main a priori hypothesis concerned the interrelationship between ventral attention network and default network, and since this is where our strongest statistical effect was observed, we sought to characterize the connectivity abnormalities involving these two networks in greater detail using circular connection graphs (see Fig. 4). There was increased connectivity in ADHD between

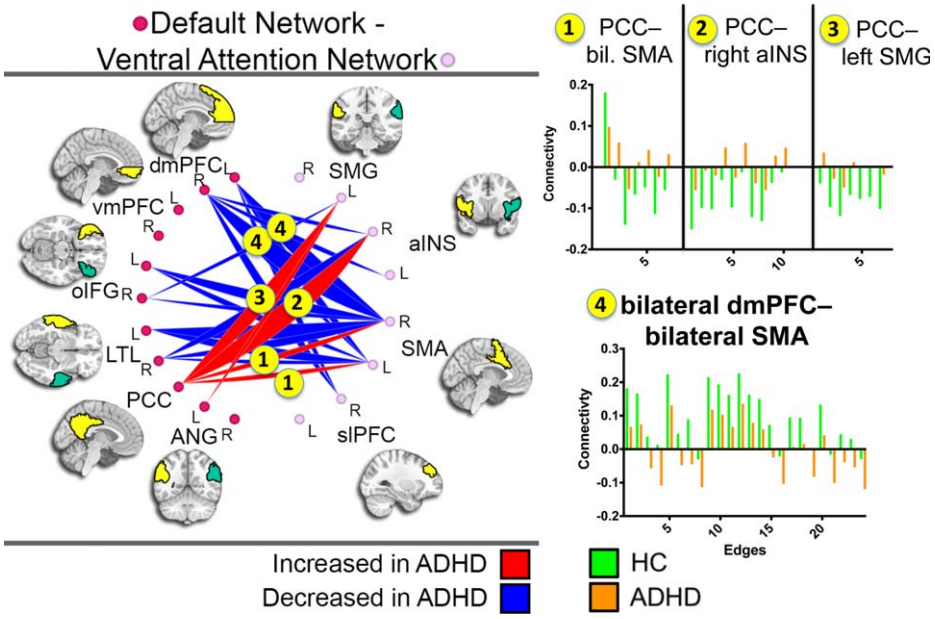

Figure 4.

Inter-region distribution of aberrant connections in ADHD. Circle graph depicts the inter-region distribution of altered connections between default network and ventral attention network. Width of each arc is proportional to the number of aberrant connections linking the two regions. There is hyperconnectivity involving SMA, right aINS, and left SMG connections with PCC, and hypoconnectivity involving SMA connections with other regions. Line graphs on right side show connectivity within each group for each implicated connection. HC, healthy control; ADHD, attention-deficit/hyperactivity disorder; bil., bilateral. Default network: dmPFC, dorsomedial PFC; vmPFC, ventromedial PFC; ANG, angular gyrus; PCC, posterior cingulate; LTL, lateral temporal lobe; oIFG, orbital inferior frontal gyrus. Not shown: medial temporal lobe. Ventral attention network: aPCN, anterior precuneus; SMG, supramarginal gyrus; aINS, anterior insula; SMA, supplementary motor area. Not shown: superior lateral PFC, precentral cortex. [Color figure can be viewed in the online issue, which is available at wileyonlinelibrary.com.]

posterior cingulate cortex in default network and three regions of ventral attention network: supplementary motor area (SMA), anterior insula, and supramarginal gyrus. Further examination of the magnitude of correlations revealed that in HCs, these connections were primarily negative. In ADHD, these anticorrelations were muted (i.e., became closer to zero or positive; Fig. 4, Graphs 1–3). Dorsal medial prefrontal cortex in default network had numerous connections with SMA. These connections exhibited a more complex pattern. In the HC group, these edges exhibited variable connectivity (both positive and negative values). In the ADHD group, these edges tended to be more negative, i.e., more weakly correlated or anticorrelated (Fig. 4, Graph 4).

For each of the five abnormal network interrelationships (i.e., the cells shaded in Fig. 2), we conducted Bernoulli tests to detect lateralization of abnormal connections. These tests identified significant right lateralization in the four cells involving the default network (see Table II). Of note, lateralization was not observed in the only cell that

TABLE II. Right lateralization of aberrant network connections

Right: network 1-network 2	*n*	Left: network 1-network 2	*n*	Bernoulli test *P* (corrected)
Right ventral attention network-default network	76	Left ventral attention network-default network	45	0.036
Right default network-visual network	94	Left default network-visual network	42	0.09
Default network-right frontoparietal network	94	Default network-left frontoparietal network	62	0.09
Right default network-right default network	98	Left default network-left default network	60	0.09

Default network exhibited aberrant connectivity with four large-scale intrinsic connectivity networks—ventral attention network, visual network, frontoparietal network, and default network (i.e., itself). The abnormal interconnections between these networks exhibited right lateralization that was statistically significant after Bonferroni correction for multiple comparisons.

did not involve the default network, i.e., the cell representing connections between frontoparietal and ventral attention network.

To assess the robustness of the network contingency analysis, we performed the analysis again using P value thresholds ranging from 0.0001 to 0.1, taking the normalized AUC of the results across analyses (see Methods for details). We found that the same five cells of the network cross-tabulation map shown in Figure 2 were statistically significant (and no other cells other than these five were statistically significant) indicating the analysis is indeed robust across P value thresholds.

An additional network contingency analysis was performed to test whether abnormal network interrelationships scaled with continuous measures of symptom severity (see Methods). This analysis found symptom severity predicted abnormal connectivity involving ventral attention network–default network ($P = 0.007$). Intradefault network connections were trend level significant ($P = 0.06$), but results were not significant for the other network interconnections.

DISCUSSION

An emerging research framework proposes that altered interrelationships between large-scale brain networks contribute to the pathophysiology of psychiatric disorders (Menon, 2011). Drawing on this perspective, we comprehensively investigated interrelationships between seven large-scale brain networks in the ADHD-200 multisite sample using connectomic methods and network contingency analysis. Consistent with recently proposed theoretical models of ADHD (Castellanos and Proal, 2012; Sonuga-Barke and Castellanos, 2007), we demonstrated ADHD brains at rest exhibit altered connectivity between key nodes of ventral attention network, which is involved in regulating attention shifts, and default network, involved in lapses of attention. Default network also exhibited distributed alterations in its interconnections with several other ICNs, and, moreover, there was pronounced right lateralization of aberrant default network connections. These findings add to growing evidence that network dysconnectivity is a central feature of ADHD (Bush, 2009; Castellanos and Proal, 2012; Cortese et al., 2013; Di Martino et al., 2013; Konrad and Eickhoff, 2010; van Ewijk et al., 2012). Moreover, this study highlights the utility of connectomic methods for comprehensively investigating distributed connectivity disturbances in psychiatric diseases.

Our finding of altered connectivity between key nodes of ventral attention network—including anterior insula and SMA—and default network is highly consistent with the findings of Castellanos et al. (2008). They observed anticorrelations between a dorsal ACC seed (within the larger region which we label "SMA") and posterior regions of the default network, and these anticorrelations were reduced or absent in participants with ADHD. We observed this same pattern as well (see Fig. 4, Graph 1). Based on previous activation studies (e.g., Weissman et al., 2006), Castellanos and colleagues also predicted a similar pattern of abnormalities in right anterior insula, which were not borne out in their data. The present study, however, supports Castellanos and colleagues' original conjecture, as we observed anticorrelations between right anterior insula and posterior default network in the HC group, which were absent in the ADHD group (Fig. 4, Graph 2). Differences in samples and methods between the two studies likely accounts for the discrepancy, e.g., we had a larger sample size (421 subjects rather than 40) and we used a connectomic method with multiple closely spaced seeds rather than a single seed. It is noteworthy that in ADHD, posterior MFC, anterior insula, and dorsal ACC also routinely exhibit abnormal activation during cognitive paradigms (Bush et al., 1999; Rubia et al., 1999, 2005, 2011; see Cortese et al., 2012 for a review). Results from the present study thus suggest that the pathology observed in these ventral attention regions in activation studies is not restricted exclusively to task but is also represented in abnormal intrinsic oscillation patterns during the resting sate.

It is useful to interpret our finding of altered interconnections between ventral attention network and default network in light of the "default network interference hypothesis," an influential model of attention dysfunction in ADHD (Sonuga-Barke and Castellanos, 2007). This model distinguishes two modes of cognitive/attention functioning, each subserved by distinct networks. The default network supports introspective orientation of attention during activities such as autobiographical memory, prospective thought, and self-related processing (Buckner et al., 2008; Raichle et al., 2001). Task positive networks, in contrast, support extrospective orientation of attention during response selection, planning, and executive processing (Corbetta and Shulman, 2002; Fox et al., 2005). These networks exhibit reciprocal relations, with activity in task positive regions associated with suppression of default network activity (McKiernan et al., 2003). Lapses of attention arise when suppression fails and default network inappropriately intrudes during externally demanding tasks (Sonuga-Barke and Castellanos, 2007; Weissman et al., 2006). Ventral attention network is a key task positive network that tracks the salience of external stimuli (Downar et al., 2000; Eckert et al., 2009; Menon and Uddin, 2010) and regulates switching between default network versus task positive modes of cognition (Menon, 2011). Evidence for this proposal comes from structural imaging (Menon and Uddin, 2010), and functional magnetic resonance imaging (fMRI) studies using activation paradigms (e.g., oddball tasks; Downar et al., 2000), functional and effective connectivity (Sridharan et al., 2008), and pharmacological manipulations (Dang et al., 2012). Our finding of aberrant ventral attention network–default network interconnections at rest in ADHD, and, moreover,

that the magnitude of these alterations is significantly correlated with ADHD symptom severity, might thus be interpreted in terms of deficient regulatory control over default network. In particular, impaired ventral attention regulation of default network in ADHD could lead to inappropriate default network intrusion during tasks and lapses of attention. In addition, given the broader role of ventral attention network in salience processing (Downar et al., 2000; Eckert et al., 2009; Menon and Uddin, 2010), ventral attention dysfunction could also contribute to more general kinds of attention dysregulation in ADHD (e.g., distractibility due to task-irrelevant stimuli).

We found diffuse hypoconnectivity throughout the default network in ADHD brains at rest (Figs. 2 and 3). This is consistent with recent reports using seed-based methods that found diminished connectivity between critical hubs of the default network (Castellanos et al., 2008; Fair et al., 2010). Other studies using various other functional imaging measures and methods—functional connectivity density mapping (Tomasi and Volkow, 2012), network homogeneity (Uddin et al., 2008), and resting state electroencephalography (EEG; Helps et al., 2008)—have also found alterations in default network in individuals with ADHD. Recently, Fair et al. (2010) have proposed that maturational lag may account for these default network abnormalities. Default network is relatively sparsely connected at ages 7–9 and becomes increasingly integrated through childhood and young adulthood (Fair et al., 2008). Concurrently, default network also becomes increasingly segregated from task positive networks (Anderson et al., 2011). If ADHD brains exhibit a lag with respect to developmental trajectory of default network connectivity, then this might account for the numerous disturbances observed in the disorder implicating this network. Of note, maturational lag has been detected in ADHD with respect to other critical behavioral and brain variables (El-Sayed et al., 2003), including cortical thickness (Shaw et al., 2007, 2013) and brain volumes (Castellanos et al., 1994, 1996; Gogtay and Giedd, 2002). In a separate report, we comprehensively investigate the developmental patterns of large-scale ICNs in the ADHD-200 sample as well as another large publicly available dataset, and we provide additional support for the maturational lag hypothesis (Sripada et al., under review).

In four of the five network pairs exhibiting altered interconnections in ADHD—in particular, the four cells in Figure 2 that involved the default network—there was significant right lateralization of abnormal connectivity. This finding is consistent with a large literature using a variety of methods—neuropsychological (Carter et al., 1995; Nigg et al., 1997; Reid and Norvilitis, 2000; Voeller and Heilman, 1988), EEG (Baving et al., 1999), perfusion imaging (Kim et al., 2002), structural MRI (Castellanos et al., 1994, 1996), and task-based fMRI (Casey et al., 1997; Depue et al., 2010)—that documents right brain deficits in ADHD. Moreover, recent circuit models implicate right brain regions in critical functions relevant to ADHD pathology. For example, right inferior frontal gyrus/anterior insula is reliably implicated in response inhibition across different cognitive domains (Aron et al., 2004; Depue et al., 2010; Smith et al., 2008) and right sided attentional networks are implicated in visual spatial attention (Corbetta and Shulman, 2002, 2011). Interestingly, right lateralized abnormalities do not appear to have been previously reported in fMRI studies of resting state functional connectivity in ADHD. This observation suggests connectomic methods such as the ones employed in this study may play a helpful role in uncovering lateralized connectivity patterns. Such patterns are likely to manifest as a skew in populations of hundreds or thousands of connections distributed over disparate brain regions—a pattern that connectomic methods can readily discover but seed-based methods might more easily miss.

In summary, using connectomic methods applied to a large multisite dataset, we demonstrate connectivity disturbances in ADHD that implicate attention control networks and default network, with significant right-lateralization of connectivity abnormalities. Our findings add to growing evidence that network dysconnectivity is a central feature of ADHD, and highlight the utility of connectomic methods for comprehensively investigating distributed connectivity disturbances in psychiatric diseases.

REFERENCES

American Psychiatric Association, American Psychiatric Association, DSM-5 Task Force (2013): Diagnostic and Statistical Manual of Mental Disorders: DSM-5. Arlington, VA: American Psychiatric Association.

Amodio DM, Frith CD (2006): Meeting of minds: The medial frontal cortex and social cognition. Nat Rev Neurosci 7:268–277.

Anderson JS, Ferguson MA, Lopez-Larson M, Yurgelun-Todd D (2011): Connectivity gradients between the default mode and attention control networks. Brain Connect 1:147–157.

ADHD-200 Consortium (2012): The ADHD-200 Consortium: A model to advance the translational potential of neuroimaging in clinical neuroscience. Front Syst Neurosci 62.

Aron AR, Poldrack RA (2005): The cognitive neuroscience of response inhibition: Relevance for genetic research in attention-deficit/hyperactivity disorder. Biol Psychiatry 57:1285–1292.

Aron AR, Robbins TW, Poldrack RA (2004): Inhibition and the right inferior frontal cortex. Trends Cogn Sci 8:170–177.

Ashburner J (2007): A fast diffeomorphic image registration algorithm. Neuroimage 38:95–113.

Baving L, Laucht M, Schmidt MH (1999): Atypical frontal brain activation in ADHD: Preschool and elementary school boys and girls. J Am Acad Child Adolesc Psychiatry 38:1363–1371.

Behzadi Y, Restom K, Liau J, Liu TT (2007): A component based noise correction method (CompCor) for BOLD and perfusion based fMRI. Neuroimage 37:90–101.

Benjamini Y, Hochberg Y (1995): Controlling the false discovery rate: A practical and powerful approach to multiple testing. J R Stat Soc Ser B Methodol 57:289–300.

Biswal BB et al. (2010): Toward discovery science of human brain function. Proc Natl Acad Sci 107:4734–4739.

Bressler SL, Menon V (2010): Large-scale brain networks in cognition: Emerging methods and principles. Trends Cogn Sci 14: 277–290.

Buckner RL, Andrews-Hanna JR, Schacter DL (2008): The Brain's Default Network. Ann N Y Acad Sci 1124:1–38.

Bullmore E, Brammer M, Harvey I, Ron M (1995): Against the laterality index as a measure of cerebral asymmetry. Psychiatry Res Neuroimaging 61:121–124.

Bush G (2009): Attention-deficit/hyperactivity disorder and attention networks. Neuropsychopharmacology 35:278–300.

Bush G, Frazier JA, Rauch SL, Seidman LJ, Whalen PJ, Jenike MA, Rosen BR, Biederman J (1999): Anterior cingulate cortex dysfunction in attention-deficit/hyperactivity disorder revealed by fMRI and the counting stroop. Biol Psychiatry 45:1542–1552.

Carter CS, Krener P, Chaderjian M, Northcutt C, Wolfe V (1995): Asymmetrical visual-spatial attentional performance in ADHD: Evidence for a right hemispheric deficit. Biol Psychiatry 37: 789–797.

Casey BJ, Castellanos FX, Giedd JN, Marsh WL, Hamburger SD, Schubert AB, Vauss YC, Vaituzis AC, Dickstein DP, Sarfatti SE, Rapoport JL (1997): Implication of right frontostriatal circuitry in response inhibition and attention-deficit/hyperactivity disorder. J Am Acad Child Adolesc Psychiatry 36:374–383.

Castellanos FX, Giedd JN, Eckburg P, Marsh WL, Vaituzis AC, Kaysen D, Hamburger SD, Rapoport JL (1994): Quantitative morphology of the caudate nucleus in attention deficit hyperactivity disorder. Am J Psychiatry 151:1791–1796.

Castellanos FX, Giedd JN, Marsh WL, Hamburger SD, Catherine A, Dickstein DP, Sarfatti SE, Vauss YC, Snell JW, Lange N, Kaysen D, Krain AL, Ritchie GF, Rajapakse JC, Rapoport JL (1996): Quantitative brain magnetic resonance imaging in attention-deficit hyperactivity disorder. Arch Gen Psychiatry 53:607–616.

Castellanos FX, Margulies DS, Kelly C, Uddin LQ, Ghaffari M, Kirsch A, Shaw D, Shehzad Z, Di Martino A, Biswal B, Sonuga-Barke EJS, Rotrosen J, Adler LA, Milham MP (2008): Cingulate-precuneus interactions: A new locus of dysfunction in adult attention-deficit/hyperactivity disorder. Biol Psychiatry 63:332–337.

Castellanos FX, Proal E (2012): Large-scale brain systems in ADHD: Beyond the prefrontal–striatal model. Trends Cogn Sci 16:17–26.

Corbetta M, Shulman GL (2002): Control of goal-directed and stimulus-driven attention in the brain. Nat Rev Neurosci 3: 201–215.

Corbetta M, Shulman GL (2011): Spatial neglect and attention networks. Annu Rev Neurosci 34:569–599.

Cortese S, Imperati D, Zhou J, Proal E, Klein RG, Mannuzza S, Ramos-Olazagasti MA, Milham MP, Kelly C, Castellanos FX (2013): White matter alterations at 33-year follow-up in adults with childhood attention-deficit/hyperactivity disorder. Biol Psychiatry 74:591–598.

Cortese S, Kelly C, Chabernaud C, Proal E, Di Martino A, Milham MP, Castellanos FX (2012): Toward systems neuroscience of ADHD: A meta-analysis of 55 fMRI studies. Am J Psychiatry 169:1038–1055.

Damoiseaux JS, Rombouts S a. RB, Barkhof F, Scheltens P, Stam CJ, Smith SM, Beckmann CF (2006): Consistent resting-state networks across healthy subjects. Proc Natl Acad Sci 103: 13848–13853.

Dang LC, O'Neil JP, Jagust WJ (2012): Dopamine supports coupling of attention-related networks. J Neurosci 32:9582–9587.

Depue BE, Burgess GC, Willcutt EG, Ruzic L, Banich MT (2010): Inhibitory control of memory retrieval and motor processing associated with the right lateral prefrontal cortex: Evidence from deficits in individuals with ADHD. Neuropsychologia 48: 3909–3917.

Di Martino A, Zuo X-N, Kelly C, Grzadzinski R, Mennes M, Schvarcz A, Rodman J, Lord C, Castellanos FX, Milham MP (2013): Shared and distinct intrinsic functional network centrality in autism and attention-deficit/hyperactivity disorder. Biol Psychiatry 74:623–632. Available at: http://www.sciencedirect.com/science/article/pii/S0006322313001765. Accessed April 9, 2013.

Downar J, Crawley AP, Mikulis DJ, Davis KD (2000): A multimodal cortical network for the detection of changes in the sensory environment. Nat Neurosci 3:277–283.

Eckert MA, Menon V, Walczak A, Ahlstrom J, Denslow S, Horwitz A, Dubno JR (2009): At the heart of the ventral attention system: The right anterior insula. Hum Brain Mapp 30: 2530–2541.

El-Sayed E, Larsson J-O, Persson H, Santosh P, Rydelius P-A (2003): "Maturational lag" hypothesis of attention deficit hyperactivity disorder: An update. Acta Pædiatrica 92:776–784.

Fair DA, Cohen AL, Dosenbach NUF, Church JA, Miezin FM, Barch DM, Raichle ME, Petersen SE, Schlaggar BL (2008): The maturing architecture of the brain's default network. Proc Natl Acad Sci 105:4028–4032.

Fair DA, Nigg JT, Iyer S, Bathula D, Mills KL, Dosenbach NUF, Schlaggar BL, Mennes M, Dickstein DP, Martino AD, Kennedy DN, Kelly C, Luna B, Schweitzer JB, Velanova K, Mostofsky S, Castellanos FX, Milham MP (2013): Distinct neural signatures detected for ADHD subtypes after controlling for micro-movements in resting state functional connectivity MRI data. Front Syst Neurosci 6:80.

Fair DA, Posner J, Nagel BJ, Bathula D, Dias TGC, Mills KL, Blythe MS, Giwa A, Schmitt CF, Nigg JT (2010): Atypical default network connectivity in youth with attention-deficit/hyperactivity disorder. Biol Psychiatry 68:1084–1091.

Fox MD, Snyder AZ, Vincent JL, Corbetta M, Van Essen DC, Raichle ME (2005): The human brain is intrinsically organized into dynamic, anticorrelated functional networks. Proc Natl Acad Sci USA 102:9673–9678.

Freedman D, Lane D (1983): A nonstochastic interpretation of reported significance levels. J Bus Econ Stat 1:292–298.

Gogtay N, Giedd J (2002): Brain development in healthy, hyperactive, and psychotic children. Arch Neurol 59:1244–1248.

Good P (2000): Permutation Tests: A Practical Guide to Resampling Methods for Testing Hypotheses, 2nd ed. New York: Springer.

Hamilton JP, Furman DJ, Chang C, Thomason ME, Dennis E, Gotlib IH (2011): Default-mode and task-positive network activity in major depressive disorder: Implications for adaptive and maladaptive rumination. Biol Psychiatry 70:327–333.

Harpin VA (2005): The effect of ADHD on the life of an individual, their family, and community from preschool to adult life. Arch Child 90 Suppl 1:i2–7.

Helps S, James C, Debener S, Karl A, Sonuga-Barke EJS (2008): Very low frequency EEG oscillations and the resting brain in young adults: A preliminary study of localisation, stability and association with symptoms of inattention. J Neural Transm 115:279–285.

Kessler RC, Adler L, Barkley R, Biederman J, Conners CK, Demler O, Faraone SV, Greenhill LL, Howes MJ, Secnik K, Spencer T,

Ustun TB, Walters EE, Zaslavsky AM (2006): The prevalence and correlates of adult ADHD in the United States: Results from the National Comorbidity Survey Replication. Am J Psychiatry 163:716–723.

Kim B-N, Lee J-S, Shin M-S, Cho S-C, Lee D-S (2002): Regional cerebral perfusion abnormalities in attention deficit/hyperactivity disorder. Statistical parametric mapping analysis. Eur Arch Psychiatry Clin Neurosci 252:219–225.

Konrad K, Eickhoff SB (2010): Is the ADHD brain wired differently? A review on structural and functional connectivity in attention deficit hyperactivity disorder. Hum Brain Mapp 31: 904–916.

Laird AR, Fox PM, Eickhoff SB, Turner JA, Ray KL, McKay DR, Glahn DC, Beckmann CF, Smith SM, Fox PT (2011): Behavioral interpretations of intrinsic connectivity networks. J Cogn Neurosci 23:4022–4037.

McKiernan KA, Kaufman JN, Kucera-Thompson J, Binder JR (2003): A parametric manipulation of factors affecting task-induced deactivation in functional neuroimaging. J Cogn Neurosci 15:394–408.

Menon V (2011): Large-scale brain networks and psychopathology: A unifying triple network model. Trends Cogn Sci 15: 483–506.

Menon V, Uddin LQ (2010): Saliency, switching, attention and control: A network model of insula function. Brain Struct Funct 214:655–667.

Nigg JT, Swanson JM, Hinshaw SP (1997): Covert visual spatial attention in boys with attention deficit hyperactivity disorder: Lateral effects, methylphenidate response and results for parents. Neuropsychologia 35:165–176.

Polanczyk G, Rohde LA (2007): Epidemiology of attention-deficit/hyperactivity disorder across the lifespan. Curr Opin Psychiatry 20:386–392.

Power JD, Barnes KA, Snyder AZ, Schlaggar BL, Petersen SE (2012): Spurious but systematic correlations in functional connectivity MRI networks arise from subject motion. Neuroimage 59:2142–2154.

Power JD, Cohen AL, Nelson SM, Wig GS, Barnes KA, Church JA, Vogel AC, Laumann TO, Miezin FM, Schlaggar BL, Petersen SE (2011): Functional network organization of the human brain. Neuron 72:665–678.

Raichle ME, MacLeod AM, Snyder AZ, Powers WJ, Gusnard DA, Shulman GL (2001): A default mode of brain function. Proc Natl Acad Sci 98:676–682.

Reid HM, Norvilitis JM (2000): Evidence for anomalous lateralization across domain in ADHD children as well as adults identified with the Wender Utah rating scale. J Psychiatr Res 34:311–316.

Rubia K, Halari R, Cubillo A, Smith AB, Mohammad A-M, Brammer M, Taylor E (2011): Methylphenidate normalizes fronto-striatal underactivation during interference inhibition in medication-naïve boys with attention-deficit hyperactivity disorder. Neuropsychopharmacology 36:1575–1586.

Rubia K, Overmeyer S, Taylor E, Brammer M, R C, Simmons A, Bullmore ET (1999): Hypofrontality in attention deficit hyperactivity disorder during higher-order motor control: A study with functional MRI. Am J Psychiatry 156:891–896.

Rubia K, Smith AB, Brammer MJ, Toone B, Taylor E (2005): Abnormal brain activation during inhibition and error detection in medication-naive adolescents with ADHD. Am J Psychiatry 162:1067–1075.

Shaw P, Eckstrand K, Sharp W, Blumenthal J, Lerch JP, Greenstein D, Clasen L, Evans A, Giedd J, Rapoport JL (2007): Attention-deficit/hyperactivity disorder is characterized by a delay in cortical maturation. Proc Natl Acad Sci USA 104: 19649–19654.

Shaw P, Malek M, Watson B, Greenstein D, de Rossi P, Sharp W (2013): Trajectories of cerebral cortical development in childhood and adolescence and adult attention-deficit/hyperactivity disorder. Biol Psychiatry 74:599–606.

Shehzad Z, Kelly AMC, Reiss PT, Gee DG, Gotimer K, Uddin LQ, Lee SH, Margulies DS, Roy AK, Biswal BB, Petkova E, Castellanos FX, Milham MP (2009): The resting brain: Unconstrained yet reliable. Cereb Cortex 19:2209–2229.

Smith AB, Taylor E, Brammer M, Halari R, Rubia K (2008): Reduced activation in right lateral prefrontal cortex and anterior cingulate gyrus in medication-naïve adolescents with attention deficit hyperactivity disorder during time discrimination. J Child Psychol Psychiatry 49:977–985.

Smith SM, Fox PT, Miller KL, Glahn DC, Fox PM, Mackay CE, Filippini N, Watkins KE, Toro R, Laird AR, Beckmann CF (2009): Correspondence of the brain's functional architecture during activation and rest. Proc Natl Acad Sci 106:13040–13045.

Sonuga-Barke EJS, Castellanos FX (2007): Spontaneous attentional fluctuations in impaired states and pathological conditions: A neurobiological hypothesis. Neurosci Biobehav Rev 31:977–986.

Sporns O, Chialvo DR, Kaiser M, Hilgetag CC (2004): Organization, development and function of complex brain networks. Trends Cogn Sci 8:418–425.

Sridharan D, Levitin DJ, Menon V (2008): A critical role for the right fronto-insular cortex in switching between central-executive and default-mode networks. Proc Natl Acad Sci USA 105:12569–12574.

Sripada C, Angstadt M, Kessler D, Phan KL, Liberzon I, Evans GW, Welsh R, Kim P, Swain JE (2014): Volitional regulation of emotions produces distributed alterations in connectivity between visual, attention control, and default networks. Neuroimage 89:110–121.

Sripada C, Kessler D, Angstadt M (under review): Lag in maturation of the brain's intrinsic functional architecture in ADHD.

Sripada CS, Kessler D, Welsh R, Angstadt M, Liberzon I, Phan KL, Scott C (2013): Distributed effects of methylphenidate on the network structure of the resting brain: A connectomic pattern classification analysis. Neuroimage 81:213–221.

Sripada RK, King AP, Welsh RC, Garfinkel SN, Wang X, Sripada C, Liberzon I (2012): Neural dysregulation in posttraumatic stress disorder: Evidence for disrupted equilibrium between salience and default mode brain networks. Psychosom Med 74: 904–911.

Tian L, Jiang T, Wang Y, Zang Y, He Y, Liang M, Sui M, Cao Q, Hu S, Peng M, Zhuo Y (2006): Altered resting-state functional connectivity patterns of anterior cingulate cortex in adolescents with attention deficit hyperactivity disorder. Neurosci Lett 400: 39–43.

Tomasi D, Volkow ND (2012): Abnormal functional connectivity in children with attention-deficit/hyperactivity disorder. Biol Psychiatry 71:443–450.

Tu P-C, Lee Y-C, Chen Y-S, Li C-T, Su T-P (2013): Schizophrenia and the brain's control network: Aberrant within- and between-network connectivity of the frontoparietal network in schizophrenia. Schizophr Res 147:339–347.

Uddin LQ, Kelly AMC, Biswal BB, Margulies DS, Shehzad Z, Shaw D, Ghaffari M, Rotrosen J, Adler LA, Castellanos FX, Milham MP (2008): Network homogeneity reveals decreased integrity of default-mode network in ADHD. J Neurosci Methods 169:249–254.

Van Ewijk H, Heslenfeld DJ, Zwiers MP, Buitelaar JK, Oosterlaan J (2012): Diffusion tensor imaging in attention deficit/hyperactivity disorder: A systematic review and meta-analysis. Neurosci Biobehav Rev 36:1093–1106.

Voeller KK, Heilman KM (1988): Attention deficit disorder in children: A neglect syndrome? Neurology 38:806–808.

Weissman DH, Roberts KC, Visscher KM, Woldorff MG (2006): The neural bases of momentary lapses in attention. Nat Neurosci 9:971–978.

Xia M, Wang J, He Y (2013): BrainNet Viewer: A network visualization tool for human brain connectomics. PLoS ONE 8: e68910.

Yeo BTT, Krienen FM, Sepulcre J, Sabuncu MR, Lashkari D, Hollinshead M, Roffman JL, Smoller JW, Zöllei L, Polimeni JR, Fischl B, Liu H, Buckner RL (2011): The organization of the human cerebral cortex estimated by intrinsic functional connectivity. J Neurophysiol 106:1125–1165.